EUROPHYSICS LETTERS 7 January 1992
Europhys. Lett., 17 (2), pp. 133-138 (1992) *published in November 1991*

One-Dimension Sub-Doppler Molasses in the Presence of Static Magnetic Field.

C. VALENTIN, M.-C. GAGNÉ, J. YU and P. PILLET
Laboratoire Aimé Cotton (*), *C.N.R.S. II*
Bât. 505, Campus d'Orsay, 91405 Orsay Cedex, France

(received 31 July 1991; accepted in final form 3 October 1991)

PACS. 32.80P – Optical cooling of atoms: trapping.
PACS. 42.50 – Quantum optics.
PACS. 42.60 – Laser systems and laser beam applications.

Abstract. – Sub-Doppler cooling has been achieved for the two closed hyperfine transitions: $F=4\rightarrow F'=5$ and $F=3\rightarrow F'=2$, of the cesium D_2 line. One-dimension optical molasses is experimentally investigated and compared for both $j\rightarrow j+1$ and $j\rightarrow j-1$ transitions, on different laser polarization configurations, in the presence, and absence of a static magnetic field. One remarkable point is that cooling is obtained with blue laser detuning for the $j\rightarrow j-1$ transition. An applied static magnetic field can also shift the sub-Doppler-cooled molasses peaks to nonzero velocities without any extra heating, for the polarization gradient configurations.

For several years now laser cooling has led to extremely low temperature in the microkelvin range for neutral atoms in optical molasses [1-3]. Theoretical understanding of cooling mechanisms exceeds the Doppler cooling frame. The sub-Doppler cooling is understood by considering a multi-level ground-state atom in the presence of a laser polarization gradient [2, 3] or a magnetic field [4-6]. Particularly, for the one-dimension configuration of two orthogonal laser polarizations (lin $\perp$ lin), the cooling mechanism has been interpreted with the Sisyphus picture [2]. Although 2D or 3D-cooling is required for most of the applications, 1D-molasses remains a system for which theoretical interpretations are the easiest ones. Moreover, the information from 1D-molasses can often be extended to 2D or 3D cases.

In this letter we report our experimental investigations on different 1D-molasses configurations. Sub-Doppler cooling has been achieved for two hyperfine transitions: $F=4\rightarrow F'=5$ and $F=3\rightarrow F'=2$ of the cesium D_2 line ($6s^2\,S_{1/2}\rightarrow 6p^2\,P_{3/2}$, $\lambda=825.1$ nm). The second case is a $j=j-1$ transition, which has never been exploited for sub-Doppler molasses, because it does not permit Doppler cooling. The purpose of this letter is to compare results obtained in the different molasses configurations for both transitions $j\rightarrow j+1$ and $j\rightarrow j-1$. We give first an experiment overview of sub-Doppler cooling induced by laser polarization gradients and by a static magnetic field in a standing wave. Then we

(*) The Laboratoire Aimé Cotton is associated with the Université Paris-Sud.

report effects due to the application of a static magnetic field to polarization-gradient molasses, leading to the manifestation of transversal molasses-drift [6, 7], recently observed for Rb atom [8]. We give a simple interpretation of these phenomena and we conclude by proposing possible applications of them.

In our experiments, a cesium atomic beam propagates through a vertical 0.3 mm wide slot of an oven heated at $\sim 100\,^{\circ}C$ and is collimated by a 3 mm diameter carbon diaphragm 75 mm away. The 1D-optical molasses is obtained 125 mm away from the oven, by two counter-propagating laser beams (one retro-reflected by a mirror). The laser beam section is $(35 \times 7)\,mm^2$. The atoms spend an average time of 135 μs inside the molasses. Quarter-wave plates are used to generate lin $\perp$ lin, or two orthogonal circular polarization (σ^+-σ^-) configuration. The entering laser beam has a maximum power of 15 mW, with the counter-propagating one attenuated by losses of a factor 6 to 20% according to the experimental arrangement. The atomic beam profile is analysed in a 22 mm range, by a 0.1 mm diameter tungsten hotwire 1.20 m away from the centre of the molasses zone. Three pairs of Helmholtz coils surround the molasses zone to compensate for the earth magnetic field, and to apply a static magnetic field if required.

The laser beam is provided by a 40 mW power c.w. single mode STC diode (slave) which is locked to a low-power single-mode Hitachi diode (master) by optical injection. The master laser is stabilized to an external confocal Fabry-Perot cavity by optical feedback. Its long-term stabilization is ensured by locking its frequency on the saturated absorption line $F = 4 \rightarrow F' = 4$ (respectively, $F = 3 \rightarrow F' = 3$) of a cesium cell. The salve laser is injected through an acousto-optic modulator, shifting the frequency on the $F = 4 \rightarrow F' = 5$ (respectively, $F = 3 \rightarrow F' = 2$) transition. The resulting laser line width is less than 100 kHz.

To put all of the atoms into the interacting hyperfine level of the ground state, $F = 4$ (respectively, $F = 3$), and to prevent leaks of atoms, we use a (20 MHz FWHM) repumping laser tuned on the $F = 3 \rightarrow F' = 4$ (respectively, $F = 4 \rightarrow F' = 4$) transition. This laser beam is perpendicular to the molasses zone and totally overlaps it. It is also retro-reflected to avoid any deviation. Its polarization is linear in the direction of the molasses-laser propagation axis.

Figure 1 summarizes the results for both $F = 4 \rightarrow F' = 5$ (*b*)-*f*)) and $F = 3 \rightarrow F' = 2$ (*g*)-*j*)) atomic transitions. All the recordings given in this letter are obtained, if not specified, with a $4\,mW/cm^2$ intensity laser beam (1.5 times the saturation value). The laser detuning is here equal in absolute value to the natural line width of the considered transition, $\Gamma \sim \sim 2\pi \times 5\,MHz$. First, all the examples of sub-Doppler molasses (fig. 1*c*)-*j*)) exhibit a narrow peak of $\sim 600\,\mu m$ FWHM superimposed on a broad pattern: either a Doppler molasses profile (fig. 1*b*)) for the $F = 4 \rightarrow F' = 5$ transition, or a laser free profile (fig. 1*a*)) for the $F = 3 \rightarrow F' = 2$ one, which presents neither Doppler cooling nor heating. For the $100\,^{\circ}C$ Cs oven, a rough estimation (1) gives a temperature of $100\,\mu K$, lower than the Doppler limit temperature $T_D = \hbar\Gamma/2k_B$ ($125\,\mu K$ for Cs). On the contrary, the Doppler profile corresponds to a temperature of $\sim 30\,mK$ higher than T_D, because the damping time is too long to permit the atoms to reach the limit temperature, especially for the high-transverse-velocity captured atoms. Furthermore, the Doppler molasses centre is shifted compared to the sub-Doppler one, due to the power imbalance between the two counter-propagating laser beams. We also notice in fig. 1*d*) that the Doppler profile in the σ^+-σ^- configuration is narrower than in the other cases, which corresponds to a stronger Doppler friction force and can be

(1) The measured widths do not depend only on the temperature but on several parameters such as longitudinal velocity distribution, molasses capture range .... We have been able to observe for higher detuning up to $250\,\mu m$ FWHM molasses peaks, corresponding to the limit of resolution of our apparatus and to a transverse temperature of $20\,\mu K$.

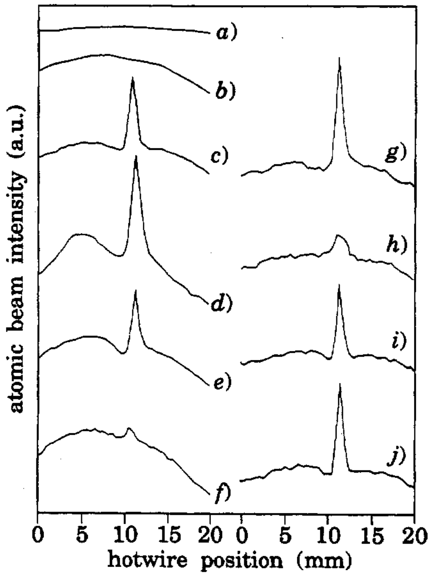

Fig. 1.

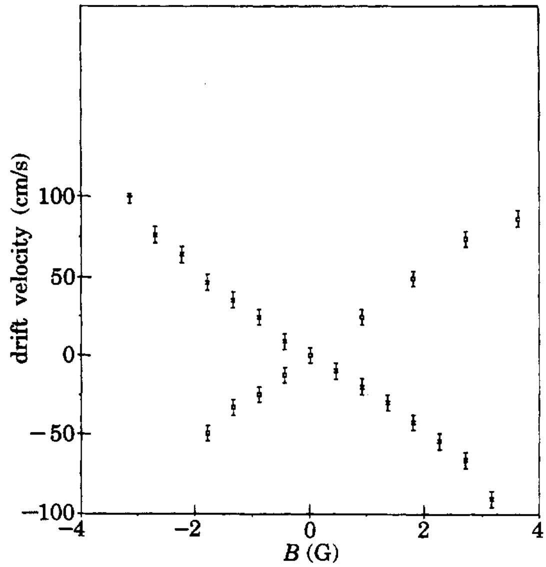

Fig. 2.

Fig. 1. – 1D-optical molasses profiles for different polarization configurations. *a)* Relatively flat transverse profile of laser free atomic beam; *b)* typical Doppler molasses profile; *c)* and *g)* polarization ellipticity gradient-induced molasses (lin ⊥ lin configuration); *d)* and *h)* motion-induced orientation molasses (σ^+-σ^- configuration); *e)* and *i)* (respectively, *f)* and *j)*) magnetic-field–induced molasses for a circularly (respectively, linearly) polarized standing wave.

Fig. 2. – Transversal drift-velocities of the σ^+-σ^- molasses peaks *vs.* magnetic field B. The crosses correspond to a -6 MHz laser detuning for the $F = 4 \rightarrow F' = 5$ transition, and the squares to a 10 MHz one for the $F = 3 \rightarrow F' = 2$ transition.

calculated. We have finally verified that the thermal equilibrium is reached for the sub-Doppler molasses, by changing the power and the detuning of the laser and the molasses interaction length.

A transversal magnetic field in a standing wave (fig. 1*e*), *f*), *i*) and *j*)) plays the same role as a laser polarization ellipticity gradient (fig. 1*c*) and *g*)). The Sisyphus force comes from the spatial modulation of the ground-state sublevel light shifts, and from the population transfers by optical pumping. In the case of a transversal magnetic field, the population transfers are the result of a competition between optical pumping and Larmor precession [5]. The Sisyphus picture can explain the magnetic-field–induced molasses, as long as the magnetic field stays weak enough.

Comparing both transitions, one remarkable difference is that a *red* detuning is required for the $F = 4 \rightarrow F' = 5$ transition and a *blue* one for the $F = 3 \rightarrow F' = 2$ one. This result appears to be general, and blue detuning seems required for cooling on the $j \rightarrow j'$ ($j' \leq j$) transitions [9]. Simple arguments based on the fact that population transfers and light shifts should correspond to energy dissipation (Raman anti-Stokes lines) mechanisms [2] can be used to explain this point. In particular, the magnetic-field–induced σ^+ molasses (cases fig. 1*e*) and *i*)) can be easily analysed. The $j \rightarrow j+1$ σ^+ molasses corresponds to a two-level system ($m_j = j \rightarrow m_{j+1} = j+1$) (the quantization axis is chosen as the laser propagation axis), and the light shift of the ground sublevel, $m_j = j$, is the largest one. The magnetic field induces population transfers from the sublevel $m_j = j$ to the other ones. To get cooling, the light shifts should be towards low energy and a red detuning is therefore required. On the contrary, for the $j \rightarrow j-1$ (respectively, $j \rightarrow j$) σ^+ molasses, the atoms are pumped into the ground sublevels, $m_j = j$ and $j-1$ (respectively, $m_j = j$), which do not interact with the laser field and are not light-shifted. The static magnetic field induces population transfers towards other sublevels which should be light-shifted towards high energy to get cooling: a blue detuning is thus required.

Finally we notice that cases fig. 1*f*) and *h*) seem to demonstrate less efficient molasses effects. It can be explained as an «incomplete» polarization of the atomic samples in the laser field, contrary to the other cases, where the population of the atoms is mostly localized on a smaller number of ground sublevels.

We present now the cases where a magnetic field is applied to a laser polarization gradient molasses. Such a situation leads to transversal molasses drift phenomena, recently pointed out in the case of Rb atom [8]. We have first applied a static magnetic field to a σ^+-σ^- molasses (cases fig. 1*d*) and *h*)) in the direction of the laser beam propagation axis ($x \parallel \boldsymbol{k}$ wave vector). We have observed a shift of the molasses peak with respect to the $v=0$ velocity position. This shift is linearly proportional to the magnetic field B. The experimental data have been taken for different laser detunings between 5 and 15 MHz in absolute value. The slope of the experimental line gives a drift velocity of ~ 28 cm/s per Gauss in absolute value (see fig. 2). The molasses peak remains narrow up to ~ 2 G and becomes broader for higher magnetic-field values. This is essentially due to the atomic beam longitudinal velocity dispersion.

The theoretical explanation for this phenomenon can be given by considering the internal atomic state in a moving (transversal velocity: v) rotating (frequency: $-kv$) frame [2]. In this frame an atom sees a linearly polarized laser field. The atom-light interaction Hamiltonian is: $-DE + kvJ_x$, where the last term is the extra inertial one due to the Larmor's theorem. The static magnetic field adds a term, $\Omega_B J_x$, to the Hamiltonian, where $\Omega_B = -g\mu B/\hbar$, μ is the Bohr's magneton, and g the Landé factor. The total Hamiltonian is $\mathcal{H} = -DE + (kv + \Omega_B) J_x$. It is easy to see that the molasses effect is no longer expected for zero velocity, but for a nonzero velocity, $v = -\Omega_B/k$ [7, 8]. The limit temperature is not changed by the presence of the magnetic field. For the transition $F=3 \rightarrow F'=2$ and $F=4 \rightarrow F'=5$, $\Omega_B/B = -2\pi \times 351$ kHz and $+2\pi \times 350$ kHz per Gauss, which gives a theoretical drift velocity of ± 29.75 cm/s/G, in good agreement with the experimental data after taking into account the precision of the longitudinal velocity. Note that the slopes for the two transitions have opposite signs, as expected.

In the lin $\perp$ lin configuration, we have applied a magnetic field along one of the laser polarization axes. The experimental data are given in fig. 3 and fig. 4. We have observed above a threshold value, B_C, of the magnetic-field absolute value, $|B|$, the splitting of the molasses signal into two peaks, symmetrically shifted from the $v=0$ position. This has also been observed for magnetic-field–induced σ-molasses [6]. In the case of the $F=4 \rightarrow F'=5$ transition, one of the two peaks is very weak and not always observable. Figure 3*a*) gives the evolution of the drift velocities of the most intense peak *vs.* B for -2 and -10 MHz laser detunings. There is no significant difference between the two curves. We observe a threshold value of ~ 1 G, then a drift velocity proportional to B with a slope of about -18 cm/s per Gauss. Figure 3*b*) gives the drift velocity curves for different values of the laser power. We note that the magnetic threshold value, B_C, decreases with the laser power ($B_C = 0.2$ G for 0.4 mW/cm^2 of laser power). For the $F=3 \rightarrow F'=2$ transition, the intensities of the two peaks are more comparable, and their shift similar in absolute value. Figure 4 shows the variation of the drift velocity *vs.* magnetic field. The results are quite similar to those of fig. 3. We observe a significant increase in the threshold value, B_C, when the laser power becomes higher.

The results obtained for the lin $\perp$ lin configuration present strong similarities with those

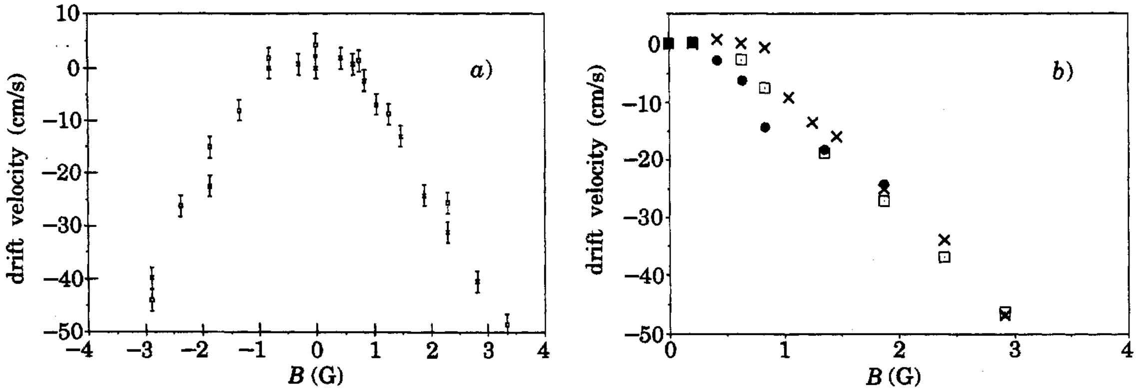

Fig. 3. – Transversal drift velocities of the lin ⊥ lin molasses peaks *vs.* magnetic field B for the $F = 4 \rightarrow F' = 5$ transition. *a*) Crosses correspond to a laser detuning of -10 MHz and the squares to one of -2 MHz; *b*) crosses correspond to laser intensity of 6 mW/cm^2, squares to 1.5 mW/cm^2, and points to 0.4 mW/cm^2.

obtained for the σ^+-σ^- configuration, and their interpretation should, therefore, also be similar. Choosing the quantization axis along the magnetic-field direction, in the moving frame (v) the atom sees a π-polarized laser beam with a frequency $(\omega - kv)$, and a σ-polarized laser beam, which is a superposition of σ^+ and σ^- polarization with a frequency $(\omega + kv)$ (ω is the laser frequency). The Larmor theorem allows us to choose a rotating frame of frequency Ω_B such that the atom no longer interacts with the magnetic field in this frame, but with a π-polarized laser beam with a frequency $(\omega - kv)$, and a superposition of σ^+ and σ^- light frequency $(\omega - \Omega_B + kv)$ and $(\omega + \Omega_B + kv)$, respectively. In this way two preferential velocities appear, $v_1 = +\Omega_B/2k$ and $v_2 = -\Omega_B/2k$, for which the molasses effect is the result of either the π-σ^+ or π-σ^- configurations. A close interpretation of this effect has been given in terms of velocity-selective resonances in ref. [8, 10].

When the magnetic field is very weak, it can be treated as a perturbation and the Sisyphus model is still approximatively valid, with the magnetic field modifying the optical pumping rates. We have even observed in our experiments a small enhancement of molasses signal (15% of total signal) at the molasses peak centre for a magnetic field of ~ 0.6 G. For

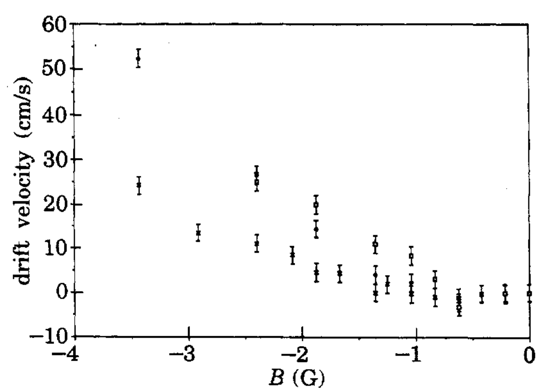

Fig. 4. – Transversal drift velocities of the lin ⊥ lin molasses peaks *vs.* magnetic field B for the $F = 3 \rightarrow F' = 2$ transition and for a laser detuning of 10 MHz. Squares, points and crosses correspond, respectively, to 1.5, 3 and 6 mW/cm^2 laser intensity.

stronger magnetic field, we can consider that the molasses is the result of a π-$\sigma^{\pm}$ configuration at a frequency $(\omega - (\pm \Omega_B)/2)$, but in the presence of the $\sigma^{\mp}$ field at a frequency $(\omega \pm 3\Omega_B/2)$. From this point of view, the two systems are not equivalent, which explains the observed differences. The quasi-disappearance of one peak is due to the presence of the $\sigma^{\mp}$ wave which perturbs the light shifts in different ways for both systems. The slope of the shifts should be half of that obtained for the σ^+-σ^- configuration: ~ 15 cm/s/G. The experimental slope in fig. 3*a*) and fig. 4 for low laser powers is approximatively 18 cm/s/G, slightly higher than the theoretical prediction. For very low laser power (fig. 3*b*)) the experimental slope (15.5 cm/s/G) is very close to the theoretical one. A rigorous treatment is presently in progress for a complete understanding of this phenomenon.

In conclusion, we have reported experimental results concerning sub-Doppler molasses in a static magnetic field, and a comparison between $j \to j+1$ and $j \to j-1$ transitions. The transversal molasses-drift results are closely related to the understanding of the magneto-optical traps [8]. The realization of sub-Doppler molasses, with a nonzero centre velocity, allows one to move a cooled atomic sample without any extra heating. It provides a new method to move atoms into an atomic trap or to make an atomic fountain, giving an alternative to the frequency or power imbalance method [11-13], and could be easier to apply in some cases.

* * *

One of the authors (M-CG) wishes to thank the Fonds pour la Formation de Chercheurs et l'Aide à la Recherche (FCAR) and the Prêt d'Honneur de la Société Saint-Jean-Baptiste du Québec for postdoctoral fellowships.

REFERENCES

[1] Lett P. D., Watts R. N., Westbrook C. I., Phillips W. D., Gould P. L. and Metcalf H. J., *Phys. Rev. Lett.*, **61** (1988) 169.
[2] Dalibard J. and Cohen-Tannoudji C., *J. Opt. Soc. Am. B*, **6** (1989) 2023; Dalibard J., Salomon C., Aspect A., Arimondo E., Kaiser R., Vansteenkiste N. and Cohen-Tannoudji C., in *Proceedings of the XI International Conference on Atomic Physics, Paris, France, 1988*, edited by S. Haroche, J. C. Gay and G. Grynberg (World Scientific, Singapore) 1989, p. 199; Salomon C., Dalibard J., Phillips W. D., Clairon A. and Guellati S., *Europhys. Lett.*, **12** (1990) 683.
[3] Shevy Y., Weiss D. S., Ungar P. J. and Chu S., *Phys. Rev. Lett.*, **62** (1989) 1118.
[4] Weiss D. S., Riis E., Shevy Y., Ungar P. J. and Chu S., *J. Opt. Soc. Am. B*, **6** (1989) 2072.
[5] Sheehy B., Shang S. Q., van der Straten P., Hatamian S. and Metcalf H., *Phys. Rev. Lett.*, **64** (1990) 858.
[6] Shang S. Q., Sheehy B., van der Straten P. and Metcalf H., *Phys. Rev. Lett.*, **65** (1990) 317.
[7] Steane A. M. and Foot C. J., *Europhys. Lett.*, **14** (1991) 231.
[8] Shang S. Q., Sheehy B., Metcalf H., van der Straten P. and Nienhuis G., *Phys. Rev. Lett.*, **67** (1991) 1094.
[9] Berman P. R., *Phys. Rev. A*, **43** (1991) 1470.
[10] Nienhuis G., van der Straten P. and Shang S. Q., *Phys. Rev. A*, **44** (1991) 462.
[11] Riis E., Weiss D. S., Moler K. A. and Chu S., *Phys. Rev. Lett.*, **64** (1990) 1658.
[12] Kasevich M., Riis E., Chu S. and de Voe R., *Phys. Rev. Lett.*, **63** (1989) 612.
[13] Clairon A., Salomon C., Guellati S. and Phillips W. D., *Europhys. Lett.*, **16** (1991) 165.